CHAPTER IV

RESULTS AND DISCUSSION

4.1 Effect of MAH loading on the grafted amount of the HDPE-*g*-MAH

The products after the reactive polymerization were slightly brown solids. The brown color can be caused by the color of MAH itself, on due to thermo-oxidative degradation of MAH under heat, oxygen and shear stress. During the extrusion, N_2 inert gas was not applied. Some thermo-oxidative degradation was expected. The graft reaction of MAH on HDPE chains is expected to produce MAH grafted HDPE as shown in Figure 4.1.

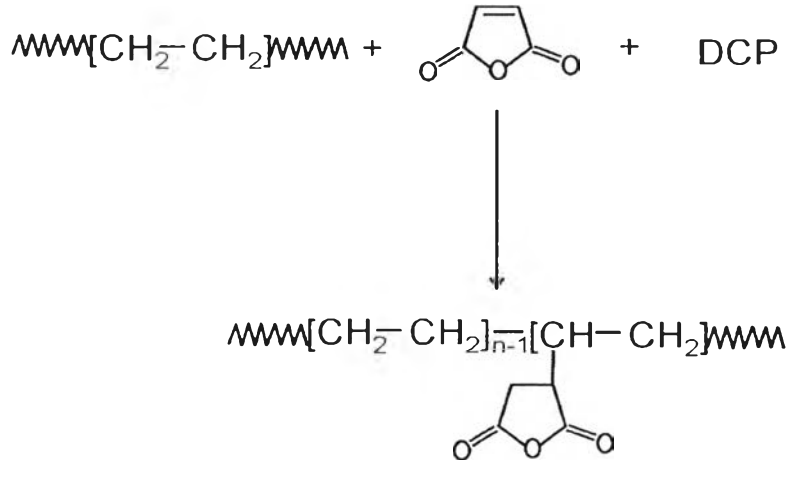

Figure 4.1 Graft reaction of MAH on HDPE chains.

Figure 4.2 shows the grafted yield of MAH grafted HDPE dependence on MAH loading, i.e., MAH loadings of 1 to 5 phr were used in the reactive melt grafting. It was found that the MAH loading of 2 phr yielded the highest grafting

degree of 1.5% onto HDPE chains. At the higher MAH loadings (3 to 5 phr), the amounts of MAH grafted HDPE were nearly constant with an unexpectedly lowest grafting yield, (0.5% yield). On the other end, the lowest MAH loading of 1 phr produced a surprisely high grafting yield (1.2%), which exceeds 100% conversion. The unusually high conversion may be caused by the impurities in MAH. At the high MAH loadings, the tendency of side reactions may increase, such as a dimerization to cyclobutane tetracarboxylic dianhydride (CBTA) under heat or degradation of the excess amount of the ungrafted MAH (Ana, Joao and Figeiro, 2008).

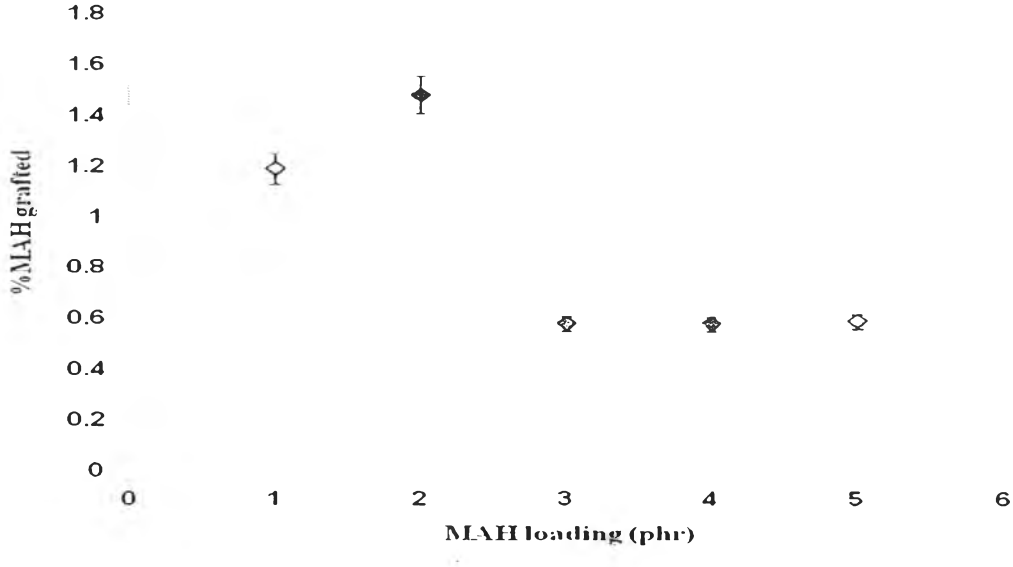

Figure 4.2 Effect of MAH loadings on grafted yields of the HDPE-*g*-MAH.

4.2 FTIR characterization

Figure 4.3 shows the FTIR spectra of the reference HDPE-*g*-MAH (commercial product), the HDPE-*g*-MAH (from the present work), MAH, and the ungrafted HDPE. New absorbance peaks at 1791 and 1716 cm^{-1} for the C=O stretching of anhydride group were observed (Moad, 1999). An intense characteristic

band at 1791 cm^{-1} and a weak absorption band at 1716 cm^{-1} are correlated with the asymmetric (strong) and symmetric (weak) C=O stretching vibrations of succinyl anhydride rings, respectively. This confirms that the grafting reaction has taken placed successfully since unreacted MAH was removed in the purification step. In Figure 4.3 also shows the peak areas of the anhydride absorption bands, which can be considered a measure of the extent of MAH grafting onto the HDPE backbone. The peak area is highest at 2 phr MAH, and drops to the low levels for the higher MAH loadings up to 5 phr. The spectra for the MAH additions at 1 and 2 phr show a new absorbance at around 890 cm^{-1} indicating the absorbance of the oxirane ring of MAH (at 865 cm^{-1} in free MAH). The peaks of –C=C– absorption of the MAH at 1603-1667 cm^{-1} disappeared in all MAH grafted HDPE spectra which indicated that the double bond was consumed in the grafting reaction and the unreacted MAH was removed by dissolution-precipitation process. The carbonyl peak of free MAH at 1772 cm^{-1} was shifted to 1791 cm^{-1} in the graft copolymer.

From the IR characterization, it is possible to confirm that the compatibilizers so prepared by reactive melt grafting between high-density polyethylene and maleic anhydride in the twin screw extruder in this work is HDPE-*g*-MAH.

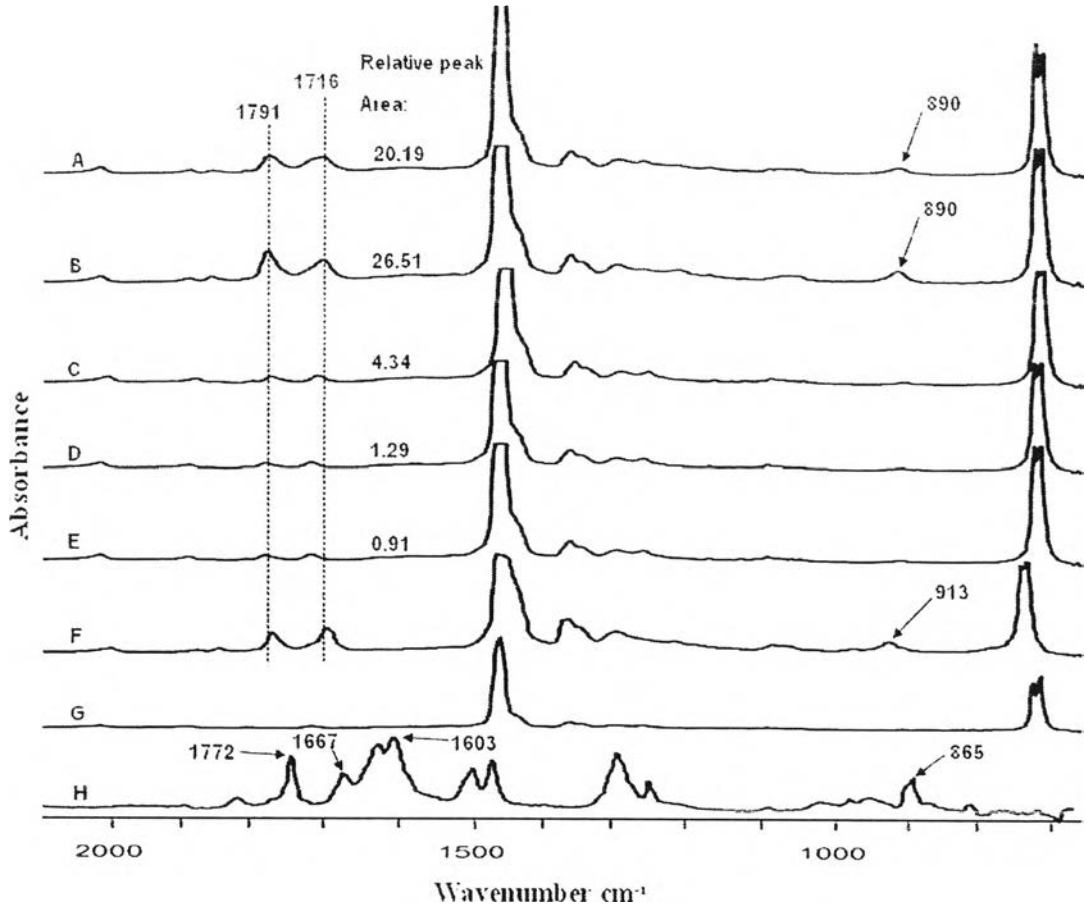

Figure 4.3 IR spectra of the currently synthesized HDPE-*g*-MAH at various MAH loadings (A : 1 phr, B : 2 phr, C : 3 phr, D : 4 phr and E : 5 phr), F : the reference PE-*g*-MAH, G is HDPE and H is the pure MAH.

Based on the new absorbance peaks at 1791 cm^{-1} and 1716 cm^{-1} for the C=O stretching from the anhydride group and at around 890 cm^{-1} assigning for the absorbance of the oxirane ring of MAH, the HDPE and MAH graft copolymerization is possible to depict in Figure 4.4.

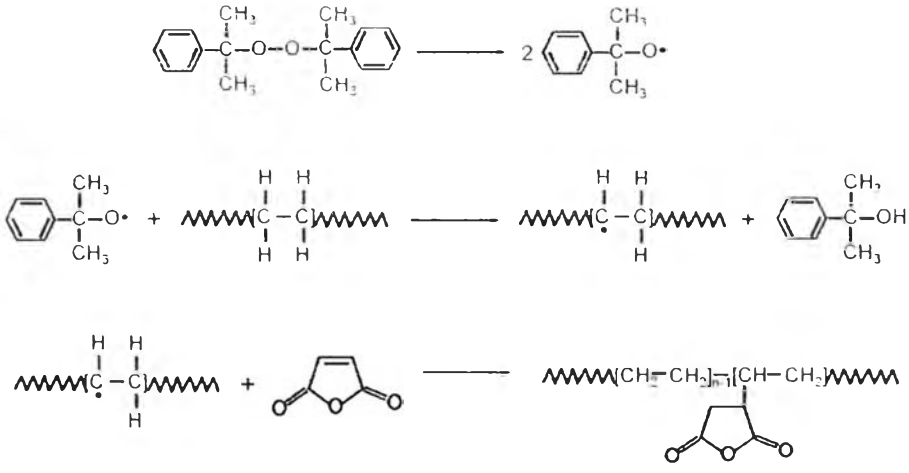

Figure 4.4 Possible grafting reaction of MAH on HDPE chains by DCP initiation.

4.3 Rheological properties of ABS/HDPE blends

The effects of blend ratio and shear rate on the shear viscosity of compatibilized ABS/HDPE blends with 1.5% MAH grafted HDPE compatibilizers are described as follows. It can be seen from Figure 4.5 that the viscosity of all the blends decreased with increases in shear rate, indicating pseudoplastic (shear-thinning) behavior of the blends. The pseudoplasticity is caused by random orientation and high entanglement of molecules. Under a high shear rate, the molecules became disentangled and oriented, resulting in a reduction of viscosity. In polymer blends, the viscosity depends on the interfacial thickness and interfacial adhesion, in addition to the characteristics of the components in the polymer.

In polymer blend, an interlayer slip along with the orientation and disentanglement takes place when increasing shear rate or shear stress. If the interfacial bonding is strong, deformation of the dispersed phase is effectively

transferred to the continuous phase. When the interfacial bonding is weak, the interlayer slip takes place easily to reduce the blend viscosity (Paul and Newman, 1978).

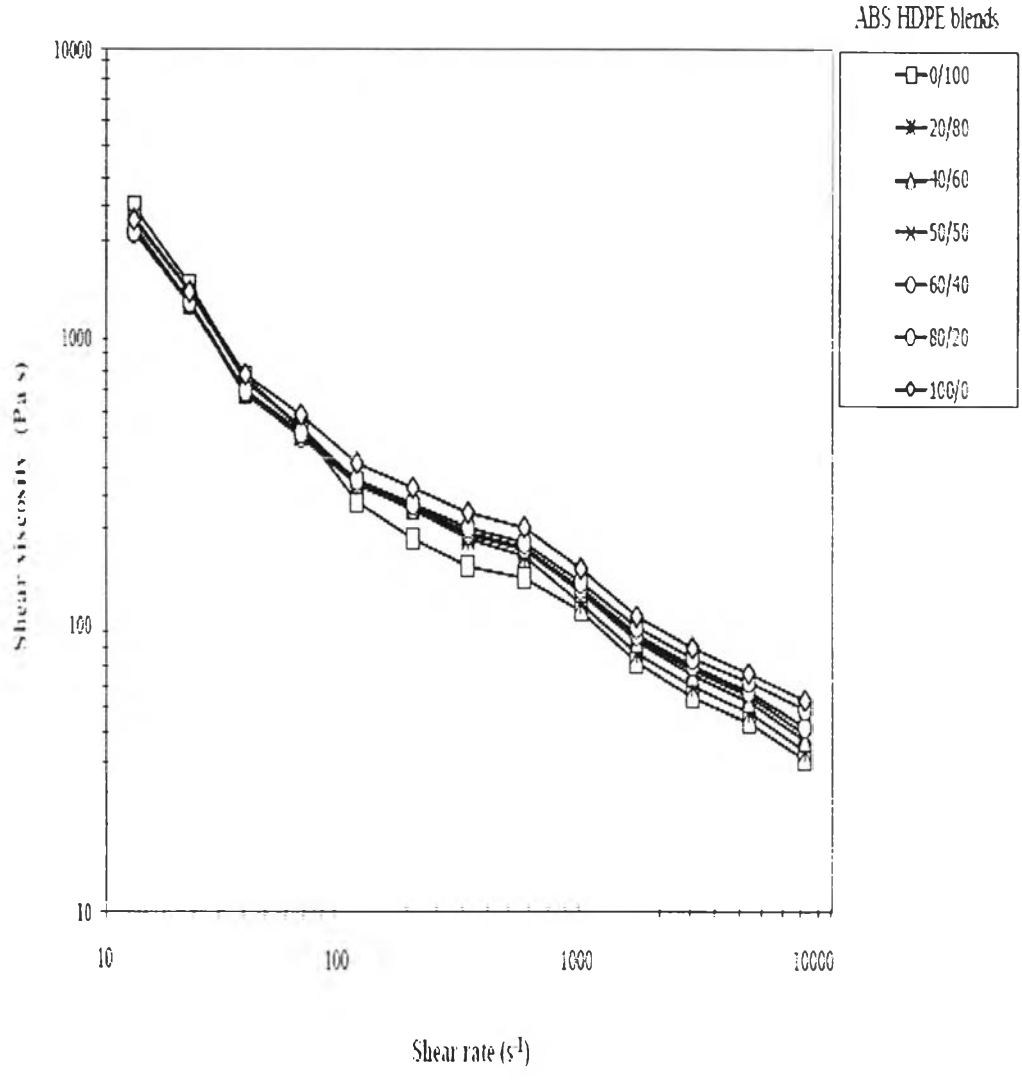

Figure 4.5 Flow curve of ABS/HDPE blends with the 1.5% HDPE-g-MAH compatibilizer.

In Figure 4.6, the shear viscosities of HDPE at the low shear rates are higher than those of ABS. At high shear rates, the shear viscosities of ABS become higher than those of HDPE. This result can be explained as follows: the compatibility of these blends is considered in terms of the viscosity ratio of the blends. If the minor component has a lower viscosity than that of the major one, the minor component will then be finely and uniformly dispersed in the major component. On the other hand, the minor component will be coarsely dispersed if its viscosity is higher than that of the major component (Paul and Newman, 1978). In the case of the ABS matrix phase and HDPE dispersed phase, the higher shear rate is required to impose HDPE dispersed phase to give the lower viscosity. The HDPE can, therefore, become finely and uniformly dispersed into the ABS matrix. The same situation can be observed in the case where ABS is the matrix and HDPE is the dispersed phase. Through this behavior, the HDPE matrix phase and the ABS dispersed phase can be compatible via this technique and with the assistance of MAH grafted HDPE. In addition, HDPE-*g*-MAH generates the lower shear viscosities at all shear rates.

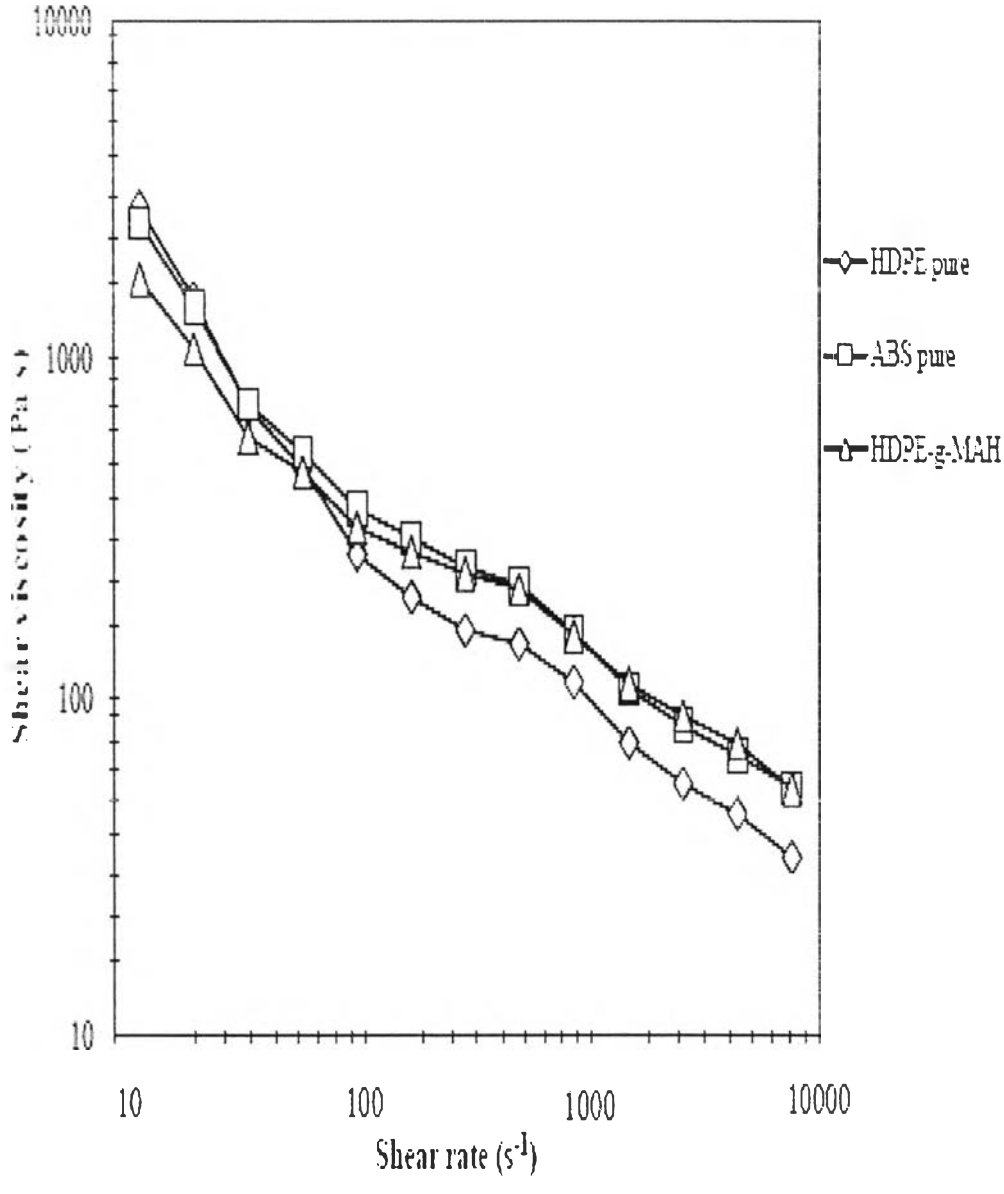

Figure 4.6 Flow curve of ABS pure, HDPE pure and HDPE-g-MAH at 473 K.

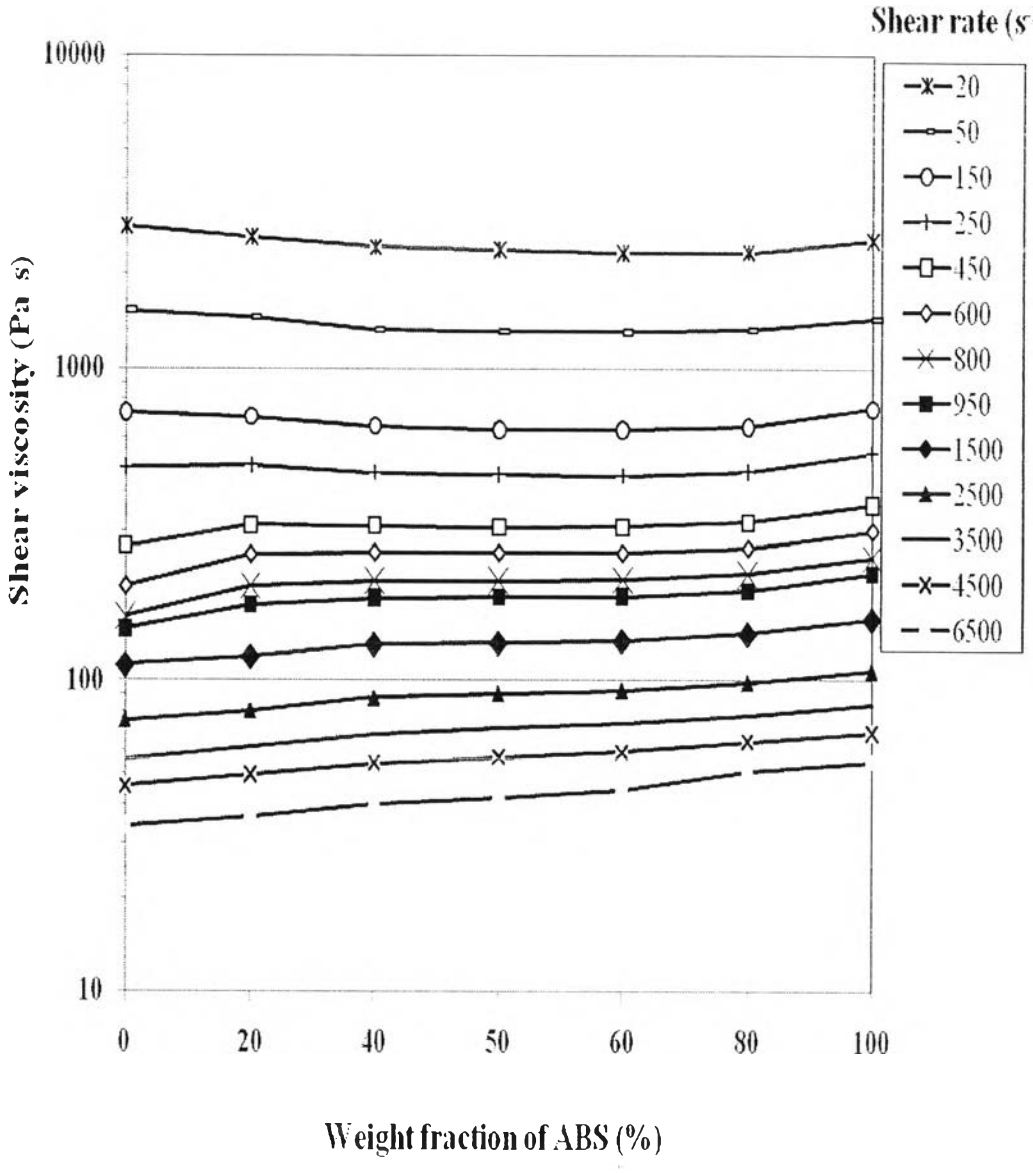

Figure 4.7 Variation of the shear viscosity as a function of weight fraction, of ABS in ABS/HDPE blends, at different shear rates.

The weight fraction of the ABS/HDPE blends against shear rate is presented in Figure 4.7. The lower shear rates (20, 50, 150 and 250 s^{-1}) give nearly constant viscosity at the blends fraction but the pure HDPE and pure ABS have the slightly

higher viscosity. When the shear rates are higher, the shear viscosities increase with increasing weight fraction of ABS. This flow patterns indicate that more compatibilization of HDPE as the dispersed phase in the higher fraction of ABS as the matrix phase had taken place with more amorphous terpolymer especially at higher shear rates. The higher shear rates and the added HDPE-g-MAH compatibilizer increased the favorable mixing of both polymers to increase interfacial adhesion and decreased each phase size.

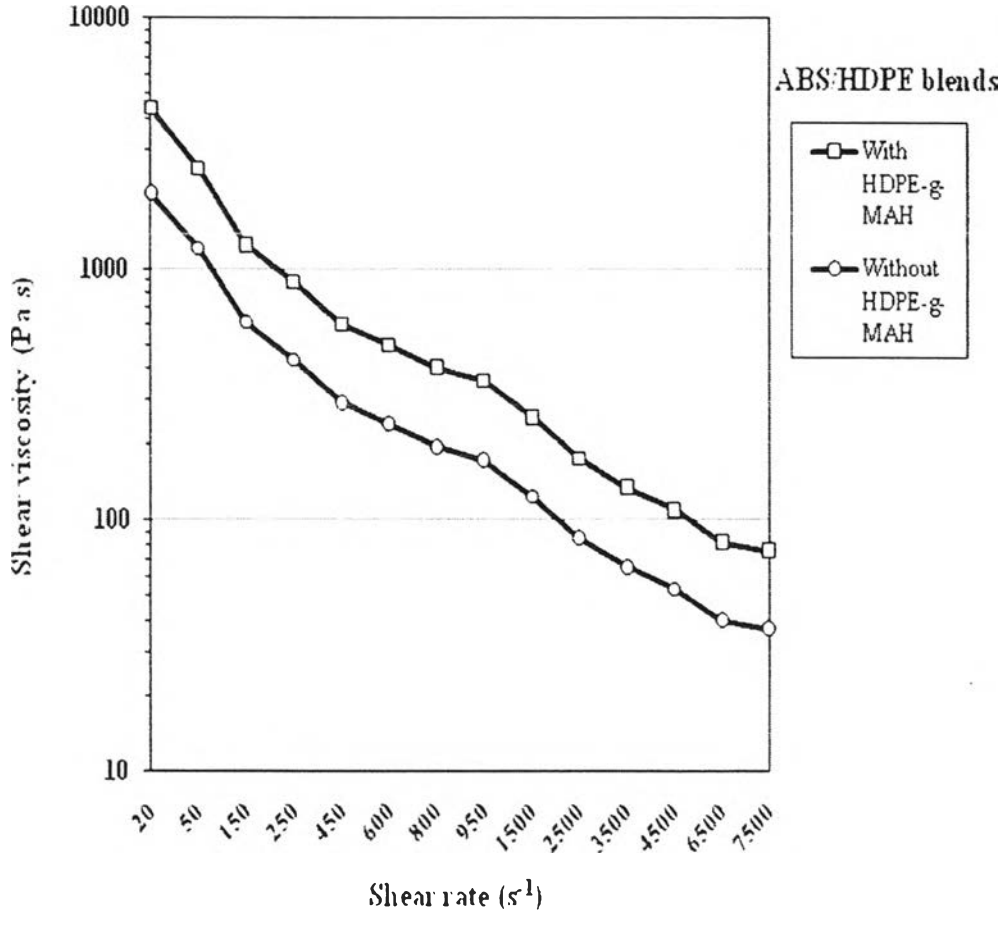

Figure 4.8 Flow curve of ABS/HDPE blends (50/50) with and without HDPE-g-MAH.

In Figure 4.8, the shear viscosity of the ABS/HDPE blends (50/50) with HDPE-*g*-MAH was higher than the blends without HDPE-*g*-MAH. At low shears, the shear viscosity of the ABS/HDPE blends (50/50) with HDPE-*g*-MAH was approximately 8 times higher than the blend without HDPE-*g*-MAH; similar trends for the middle and high shear rates, a 6 times higher the shear viscosity than the blend without HDPE-*g*-MAH are also observed.

The strong or weak interactions between phases of the blend can be determined by a positive or negative deviation of the measured viscosity from that calculated by the log additivity rule model. It is used for the evaluation of the thermodynamic compatibility of the polymer blend for the deviations of the blend viscosities from the ideal behavior.

The results of compatibility analysis by log additivity rule model are shown in Table 4.1. In relation to log additivity rule model, the ABS/HDPE blend ratios from 20/80 to 80/20 showed the slightly negative deviation behavior (NDB) at low and a positive deviation behavior (PDB) at high shear rate. This indicates incompatibility at the low shear rates, and the two components become more compatible at the high shear rates.

Table 4.1 Shear viscosity of ABS/HDPE blends compatibilized with HDPE-g-MAH from experimental data versus log additivity rule model.

ABS/HDPE	Shear rate (s^{-1})	HDPE-*g*-MAH (2 phr)		Status of deviation behavior
		Log η blend	Log η Eq 2.2	
20/80	150	2.84	2.86	Slightly negative
	600	2.40	2.34	Slightly positive
	1500	2.08	2.08	Slightly positive
	4500	1.71	1.70	Slightly positive
	6500	1.59	1.58	Slightly positive
40/60	150	2.81	2.86	Slightly negative
	600	2.41	2.37	Slightly positive
	1500	2.12	2.11	Slightly positive
	4500	1.73	1.73	Slightly positive
	6500	1.63	1.62	Slightly positive
50/50	150	2.80	2.86	Slightly negative
	600	2.41	2.39	Slightly positive
	1500	2.12	2.13	Slightly negative
	4500	1.75	1.75	Slightly positive
	6500	1.65	1.64	Slightly positive
60/40	150	2.80	2.86	Slightly negative
	600	2.41	2.41	Slightly positive
	1500	2.13	2.14	Slightly negative
	4500	1.77	1.76	Slightly positive
	6500	1.67	1.66	Slightly positive
80/20	150	2.81	2.87	Slightly negative
	600	2.42	2.44	Slightly negative
	1500	2.15	2.17	Slightly negative
	4500	1.80	1.80	Slightly positive
	6500	1.71	1.70	Slightly positive

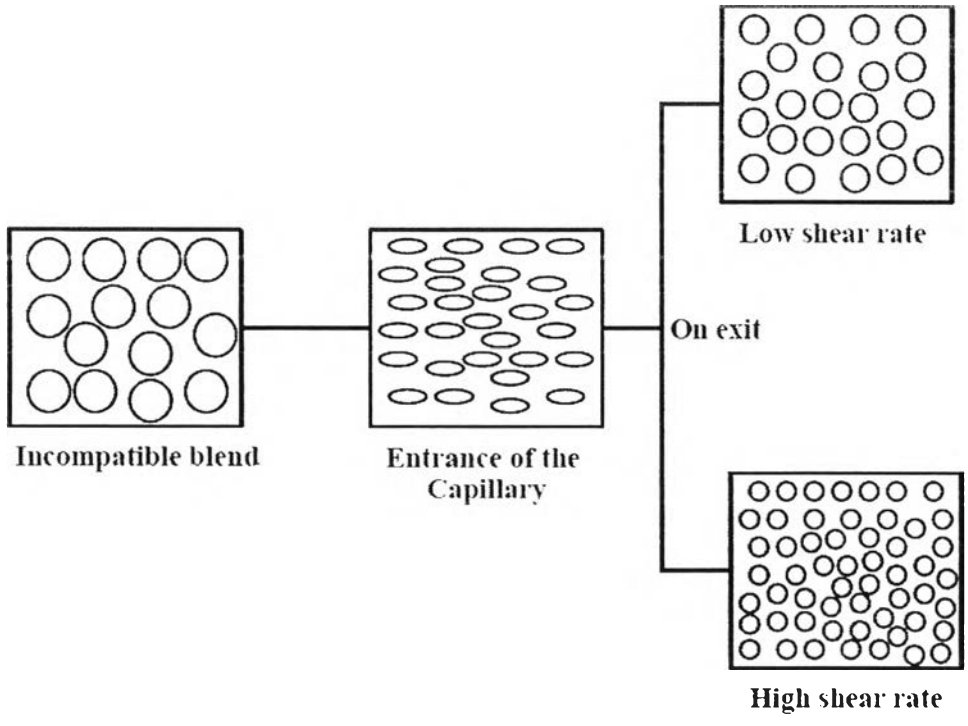

Figure 4.9 Illustrative model indication of particles break down of an incompatible blend at different shear rates in a capillary during extrusion.

A schematic explanation of the incompatible blend ABS/HDPE was sheared in the capillary rheometer under low and high shear rates in the capillary rheometer is shown in Figure 4.9. Compared with Table 4.1, one can observe that most blends are more compatible at the higher shear rates than those at the lower shear rates. At high shear rate, the dispersed phase is composed of very minute droplets, the compatibilizers enhances better dispersion, hinders coalescence and aggregation of the dispersed phase and thus improving interfacial wetting and adhesion between the two polymer phases.

4.4 Morphological observation of ABS/HDPE blends

The morphology of compatibilized blends of ABS/HDPE (50/50) with HDPE-*g*-MAH as compatibilizers prepared in a counter-rotation twin screw extruder are shown in Figure 4.10. The effects of compatibilizer concentration on blend morphology were examined in a 50/50 ABS/HDPE blend with 0, 2, 4, 8 phr of HDPE-*g*-MAH. As mentioned in the section 3.7 that the etched samples were obtained from the etching of toluene of the fractured surfaces of the samples. Since the total solubility parameters (δ_T) of HDPE, ABS and toluene are 16.3, 23.0 and 18.2 $MPa^{1/2}$, respectively, whereas those of PB = 18.0, PAN = 23.0, and SAN = 22.7 $MPa^{1/2}$ (Ping, Baoli, Lina, and Bin, 2010). Based on the total solubility parameter, it can be said that toluene is a relative good solvent for HDPE and a very good solvent for PB portion of the ABS phase, thus the HDPE surface and PB portion shall be removed (Ramirez, Sandoval, Hernandez, Martinez and Sanchez, 2005) and the phase remained and presented should be the components composing of ABS phase. Figures 4.10A and 10B are the neat HDPE and ABS; there are a very small change on theirs surfaces; whereas Figures 4.10C to 4.10F are the etched and toluene extracted surfaces under the compatibilizing influences of HDPE-*g*-MAH. Since the HDPE phase (δ = 16.3 $MPa^{1/2}$) and the portion of PB (δ = 18.0 $MPa^{1/2}$) in ABS should be removed by toluene (δ = 18.2 $MPa^{1/2}$) extraction. Figures 4.9C shows the coarse continuous phase of ABS (the long strands of PAN and SAN phases) and poor interfacial adhesion between phases because of no HDPE-*g*-MAH addition. A small decrease in particle size was observed with the incorporation of 2 phr of the compatibilizer in Figure 4.10D. The dispersions of PAN or SAN in the ABS/HDPE blends in Figure 4.10E and F were much finer when the compatibilizer concentration

increased (4 and 8 phr) because of the better interfacial adhesion. Based on the above mentioned morphologies, the optimum HDPE-*g*-MAH addition should be 4 phr.

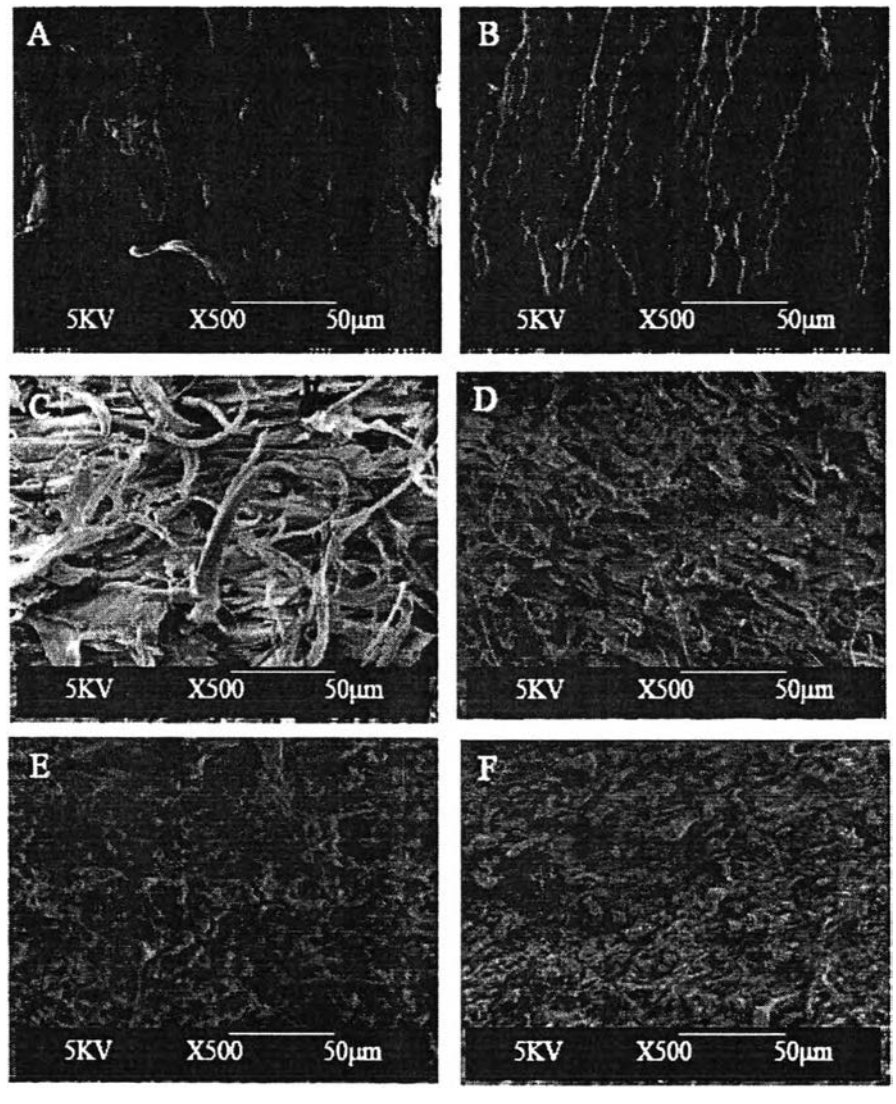

Figure 4.10 Scanning electron micrographs showing etched impact fracture surfaces of A) neat HDPE, B) neat ABS, C) ABS/HDPE (50/50) blends without HDPE-*g*-MAH, D) ABS/HDPE (50/50) blends with HDPE-*g*-MAH 2 phr, E) 4 phr, and F) 8 phr.

4.5 Thermal Analysis of ABS/HDPE blends

Thermal analysis of the ABS/HDPE blends is shown in Table 4.2. In general, the glass transition temperature of styrene in ABS is 382.5 K. In ABS, the mineral oil is added as a plasticizer for adjusting the melt flow index. Such an addition of the mineral oil is to increase the free volume of the polymer system, to give more polymeric segmental motion, which leads to reducing in the T_g. When ABS is blended with the HDPE at various portions in the ABS-rich phase, the added HDPE behaved as a disperse phase, which reduced the free volume of the system leading to an increase in the ABS continuous phase. The compatibilization of ABS/HDPE blends did not show any appreciable shift in T_g values. This indicates that the addition of 2 phr HDPE-*g*-MAH as a compatibilizer maintained the marginal level of miscibility. The data in Table 4.2 imply that the DSC did not detect any glass transition of the HDPE portion but only detected the ABS part since the values shown are the glass transition of the ABS phase. As a matter of fact, to produce the good T_g of this system that contains PE portion that has a very weak glass transition, a special type of double-furnace DSC is needed. The double-furnace DSC used ultra light weight furnaces with very low thermal inertia can achieve the fastest possible DSC response time to detect the changes in glassy state of polymers. It allows very fast controlled linear heating and cooling scanning up to 750 K min^{-1} (Norman and Ye, 2011).

Table 4.2 T_g and T_m of ABS/HDPE blends compatibilized with HDPE-g-MAH (2 phr).

ABS/ HDPE	T_g (K)	T_m (K)
100/0	382.5	-
0/100	162*	404.1
80/20	383.7	405.0
60/40	382.8	403.7
50/50	383.5	404.8
40/60	ND	406.6
20/80	ND	405.8

* = The T_g of the HDPE sample measured by HyperDSC (Perkin Elmer8500) to be approximately -111.63 °C (162 K), Cp = 0.014 J/g with a heating rate of 100 K min^{-1} (Norman and Ye, 2011). ND = Not detectable.

The thermal properties of the blends in the crystalline, melting properties are listed in Table 4.3, it can be seen that, there is a slight difference in crystallization between the HDPE and the blends could be related with the fact that HDPE has higher crystallinity; nevertheless, these differences in crystallinity are relatively low (Ramirez, Sandoval, Hernandez, Martinez and Sanchez, 2005). The ABS/HDPE blends with the incorporation of HDPE-g-MAH did not appreciably affect T_c and T_m properties of the blends.

Table 4.3 Thermal properties of the blends components.

ABS/HDPE-*g*-MAH/HDPE	Exothermic			Endothermic		
	T_c (K)	ΔH_c (J/g)	Crystallinity (%)	T_m (K)	ΔH_m (J/g)	Crystallinity (%)
0/0/100	388.5	185.2	63.2	404.4	-171.6	58.6
100/0/0	388.3	1.83	0.6	410.1 382.7	-1.2 -1.6	0.44 0.65
20/2/80	386.6	122.4	41.8	405.8	-110.9	37.9
40/2/60	387.1	97.4	33.3	406.6	-91.6	31.3
50/2/50	386.6	71.8	24.5	407.1	-64.2	21.9
60/2/40	389.2	69.4	23.7	403.7	-66.1	22.5
80/2/20	388.0	27.5	9.4	405.0	-27.6	9.4
50/0/50	388.1	82.2	28.1	404.8	-80.6	27.5

4.6 Mechanical properties of ABS/HDPE blends

Generally, it has been known for a long time that immiscible polymer blends have interior mechanical properties due to the existence of weak interfacial adhesion and poor dispersion of the component. In this study, the mechanical properties for the compatibilizing effect of ABS/HDPE blends by HDPE-*g*-MAH on the impact strength, tensile strength and flexural strength are investigated.

4.6.1 Impact strength of ABS/HDPE blends

Izod impact strength data of ABS/HDPE blends compatibilized with and without HDPE-*g*-MAH are shown in Table 4.4.

Table 4.4 Mechanical properties of ABS/HDPE blends with HDPE-*g*-MAH.

ABS/HDPE	HDPE-*g*-MAH phr	Izod impact strength ($J\ m^{-1}$)	Tensile strength (MPa)	Elongation at break (%)	Flexural strength (MPa)
100/0	0	20.0 ± 1.32	34.0 ± 3.14	50.0 ± 3.34	63.0 ± 0.23
0/100	0	22.5 ± 1.03	45.0 ± 5.15	160.2 ± 3.94	17.0 ± 0.10
80/20	0	4.7 ± 0.04	29.8 ± 2.27	13.2 ± 1.12	25.2 ± 0.17
80/20	2	7.7 ± 0.04	31.5 ± 2.74	60.2 ± 2.12	37.2 ± 0.27
50/50	0	3.4 ± 0.16	23.9 ± 2.12	11.2 ± 1.75	23.8 ± 0.14
50/50	2	6.4 ± 0.72	25.2 ± 1.56	71.2 ± 2.45	20.3 ± 0.15
20/80	0	6.2 ± 0.26	27.4 ± 2.29	107.0 ± 2.18	20.6 ± 0.33
20/80	2	12.2 ± 0.39	28.8 ± 2.45	137.0 ± 2.60	16.6 ± 0.47

Number of mechanical testing is 5.

It can be seen that the Izod impact strengths of all uncompatibilized blends became poor because of the poor interfacial adhesion between the two phases. When they were compatibilized by HDPE-*g*-MAH, the impact strength was improved and increased in each blend ratio. The impact strength of the compatibilized blends increased slowly with HDPE contents in the blends was less than that of 50/50 blend. When the HDPE became the continuous phase, the impact strength was sharply increased with increasing HDPE contents which was in good agreement with those of

Tjong and Xu (1998). The HDPE matrix phase (>50 wt %) might be more compatible with HDPE-*g*-MAH than the ABS matrix phase.

4.6.2 Tensile strength of ABS/HDPE blends

Tensile strength data of ABS/HDPE blends uncompatibilized and compatibilized shown in Table 4.4 indicate that the compatibilized blends yield the higher values than the uncompatibilized blends. The tensile strength was improved and increased about 5%in each blend ratio.

Elongation at break results also shows that the uncompatibilized blends yield lower values at all blends. It is because ABS is a hydrophobic polymer, which cannot be miscible in the HDPE matrix. The elongation at break for all blend ratios illustrates the result of poor dispersibility of ABS domains in the HDPE matrix polymer. When the blend ratio of ABS/HDPE is 20/80, the elongation at break of the blends is influenced by the effect of the HDPE matrix polymer. HDPE is a low modulus and ductile material with a relatively high degree of crystallinity (63.2%). However, these blends were influenced by ABS since the elongation at break was lower than that of neat HDPE. For the compatibilized blends, the elongation at break increased because of the influence of the crystallinity portion of HDPE.

4.6.3 Flexural strength of ABS/HDPE blends

The flexural strengths of the neat ABS and ABS blends as a continuous phase without the compatibilizer are higher than the neat HDPE and HDPE blends as a continuous phase as shown in Table 4.4. It seems that incorporation of the compatibilizers at 2 phr cannot improve the strength at all blend ratios. It is anticipated that the low flexural strength of HDPE plastics is an inherent property of the high crystallinity plastics. As shown in Table 4.4, increasing the HDPE weight fraction, the strength decreased steadily. Therefore, more loading of HDPE-*g*-MAH, such as, 4 phr or more should be needed to improve the flexural strength of the blends.

4.7 Weathering properties of ABS/HDPE blends

The weather stability was also examined by monitoring the color difference ΔE for yellowness as shown in Table 4.5. It can be seen that the ΔE value of the neat ABS is highest as an inherent property because the thermo-oxidative degradation occurs more readily in the rubber phase (polybutadiene phase), leading to chain scission and formation of hydroperoxides. Degradation was believed to occur by hydrogen abstraction from the α-carbon next to the trans-1, 4 and 1, 2 unsaturations in the polybutadiene phase (Tiganis, Burn, Davis and Hill, 2002). The ΔE values of all of blend ratios decreased with increasing the HDPE contents, while the neat HDPE has the lowest ΔE of yellowness. It can be explained that the HDPE has a greater proportion of crystalline regions, the size, and size distribution of crystalline regions are determinants of environment resistance. In addition, ΔE of

yellowness increased with increasing exposure times from 100 h to 300 h. The neat HDPE after 100 h of weathering test did not produce any appreciable ΔE value, human eye cannot differentiate the change of color when $\Delta E < 1$.

Table 4.5 ΔE of Yellowness of ABS/HDPE blends compatibilized with HDPE-*g*-MAH after weathering test 100 h, 200 h and 300 h.

ABS/HDPE	HDPE-*g*-MAH phr	ΔE of yellowness		
		100 h	200 h	300 h
100/0	2	5.62 ± 0.20	11.31 ± 0.19	14.41 ± 0.16
0/100	2	0.91 ± 0.15	3.52 ± 0.16	3.82 ± 0.11
80/20	2	3.84 ± 0.17	10.54 ± 0.23	13.91 ± 0.22
60/40	2	3.23 ± 0.12	9.15 ± 0.17	13.06 ± 0.21
50/50	2	2.60 ± 0.20	8.34 ± 0.10	11.80 ± 0.22
40/60	2	2.46 ± 0.18	7.31 ± 0.11	10.84 ± 0.18
20/80	2	1.99 ± 0.21	6.16 ± 0.13	8.45 ± 0.16